OCEANOLOGY, 2025, Vol. 65, No. 1, pp. 155–165

MARINE GEOLOGY

ESTIMATING OF CHANGES IN THE VOLUME OF SANDY BEACH DURING A STORM

© 2025 I. O. Leont'yev*

Shirshov Institute of Oceanology, Russian Academy of Sciences, Moscow, Russia

**e-mail: igor.leontiev@gmail.com*

Received July 22, 2024
Revised July 30, 2024
Accepted October 03, 2024

Abstract. An approach is proposed for predicting storm-induced changes in subaerial volume of a sandy beach based on the author's model of sediment transport in the swash zone. Input parameters in the model are the mean sand size, the slope of the beach and a chronogram of heights and periods of waves in deep water. To calibrate the model, published data from experiments in wave channels were used. Verification of the model was based on the published data from field observations. It is shown that on profiles with a developed system of nearshore bars, beach changes are small even during strong, prolonged storms, while on shores without bars or with one bar, storm erosion is measured in tens of cubic meters per meter of shore. From the calculations it follows that in the intensifying phase of the storm, the slope and volume of the beach decrease, and in the attenuation phase, on the contrary, they increase. Adaptation to external influences occurs with a certain time lag. Changes to the beach under the influence of two successive storms of approximately equal strength are largely determined by the first of them. The root mean square error of the calculations ranges from 11 to 24% relative to the average value of recorded changes in beach volume.

Keywords: *wave runup, swash zone, sediment transport, storm scenario, beach erosion and accretion, equilibrium beach slope*

DOI: 10.31857/S00301574250113e6

INTRODUCTION

A sea beach is an element of coastal relief, which performs the function of coastal protection from storm impacts. As a result of wave transformation and breaking in the surf zone near the shoreline, a swash flow with significant velocities is formed. Its energy is absorbed mainly by the over-water part of the beach above the mean water level. During the impact of the surge, beach volume can decrease or increase, depending on the phase of the storm cycle. During storm intensification, scour tends to dominate, while partial or complete recovery is possible during storm attenuation. Sometimes losses of beach material exceed a critical mark and become irreversible, which leads to progressive degradation of the coast as a whole [5, 21].

Thus, predicting the resulting changes in beach volume over the period of a storm cycle or their series is a highly relevant problem. This determines a significant interest in the study of dynamic processes in the swash zone and their modeling [10–13]. At present, several models of beach dynamics aimed at practical application are known [16, 18, 24]. Their review and comparison on the basis of experiments in wave channels are given in [14]. There, an improved version of the most suitable, in the authors' opinion, model [18] is proposed, which, in general, correctly reproduces the changes in the beach profile and volume recorded in laboratory conditions under constant parameters of wave action. However, the calculations have not yet been compared with field data, and the possibility of applying this model to real storm conditions with variable wave characteristics remains questionable.

The aim of this paper is to justify a fairly simple method for predicting changes in the volume of the overwater part of a sandy beach under the influence of a given storm, including the amplification, maximum and attenuation phases. It is based on a model of sediment transport in the wave swash zone developed by the author [1, 20], in which a number of additional options are introduced. Changes in beach volume are determined using the law of conservation of mass. The model parameters are calibrated on the basis of published data from experiments in wave channels. The results of the calculations are compared with

published data from field observations, during which storm scenarios and the corresponding resulting beach changes were recorded

MODEL CONCEPT

Wave swash zone dynamics

The swash zone comprises an overwater and an underwater part, bounded respectively by the runup height R and a certain depth h_s (Fig. 1a). It is assumed that the sediment discharge q_R in the swash zone reaches its maximum value $\hat{q}_R$ at the water's edge, and as we approach the zone's boundaries its absolute value decreases and tends to zero. For the sake of simplification, we assume that in the overwater part of the beach the discharge decreases linearly, $q_R = \hat{q}_R \dfrac{l_R - x}{l_R}$, i.e., with a constant gradient $\dfrac{dq_R}{dx} = -\dfrac{\hat{q}_R}{l_R}$. Here x is the horizontal distance, which is counted towards the shore, $l_R = R/\beta$ is the length of the overwater part of the swash zone, $\beta = \tan\alpha$ is the average slope of the beach, where the angle α is assumed to be sufficiently small ($\cos \approx 1$).

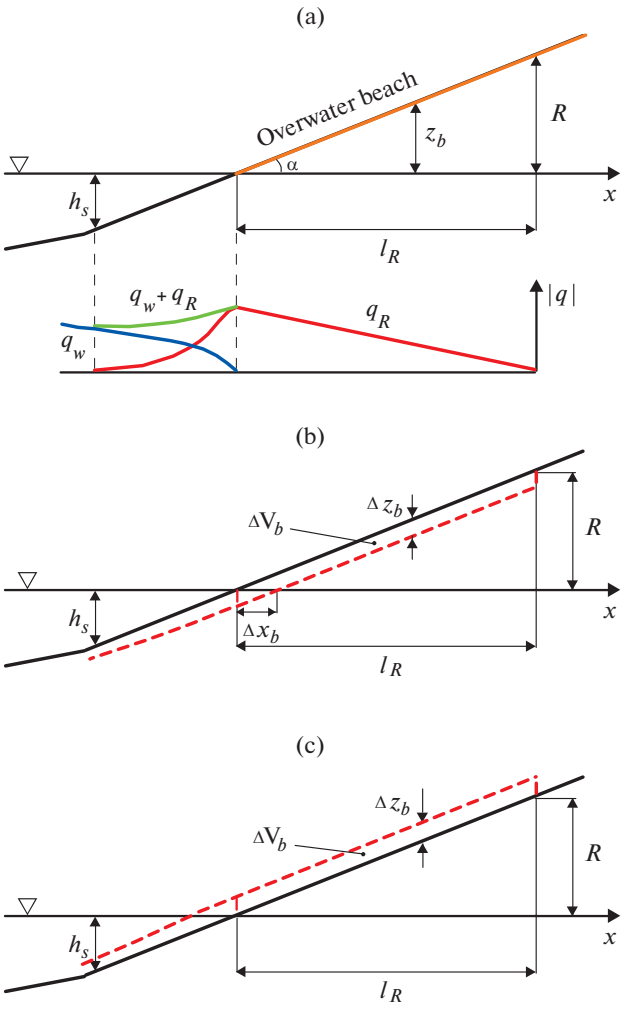

Fig. 1. Schematic of the beach and distribution of sediment discharge in the swash zone (a); beach deformation under erosion (b) and accumulation (c). Notations in the text.

From the law of conservation of mass we have

$$\frac{dz_b}{dt} = -\frac{dq_R}{dx}. \qquad (1)$$

Consequently, the elevation of the beach z_b during the time Δt changes by the amount $\Delta z_b = \dfrac{\hat{q}_R}{l_R}\Delta t$, and the changes in the volume of the overwater beach are

$$\Delta V_b = \Delta z_b l_R = \hat{q}_R \Delta t. \qquad (2)$$

In the underwater part of the swash zone, q_R decreases to zero. However, there is already sediment transport q_w, driven by wave mechanisms, and the values of q_R and q_w add up (Fig. 1a). Wave mechanisms transport sediment from the beach to the submarine slope during erosion or in the opposite direction during accumulation. As for the depth h_s, corresponding to the lower boundary of the swash zone, it is considered as a function of wave parameters [1, 2] or runup height [14].

The schemes in Figs. 1b and c reflect the situations of beach erosion and accretion. The boundaries of the deformation areas are conventionally shown with vertical lines, although in fact the bottom slopes here should be close to the limiting value (for sand about 0.6).

Total changes in overwater beach volume V_b over the storm cycle period T_w are calculated by summing the values of ΔV_b for all consecutive time steps:

$$V_b = \sum_{i=1}^{N} \Delta V_{bi}, \quad N = T_w / \Delta t. \qquad (3)$$

The step Δt of the time series characterizing the changes of wave parameters during the storm was taken as 3–6 h.

The key element of the model is the sediment discharge $\hat{q}_R$, which is defined in the next section.

Sediment discharge formula

The swash flow is characterized by the reciprocating motion of the water mass on the beach surface. Assuming that solid particles here move mainly by saltation, we apply the well-known Bagnold's formula [9] for the bed-load transport rate:

$$q_R^+ = \frac{\varepsilon_b (\tau u)^+}{\tan\phi + \beta}, \quad q_R^- = \frac{\varepsilon_b (\tau u)^-}{\tan\phi - \beta}. \qquad (4)$$

Here, the rates q_R^+ and q_R^-, expressed in units of submerged sediment weight, refer to the forward and reverse swash flows, $\varepsilon_b \approx 0.1$ is the sediment transport efficiency factor, τ is the bottom shear stress, u is the flow velocity, $\tan\phi \approx 0.6$ is the coefficient of friction of solids in horizontal shear, and β is the bottom slope. The values $(\tau u)^+$ and $(\tau u)^-$ express the rates of energy dissipation in forward and reverse flows, with $(\tau u)^+ + (\tau u)^- = (\tau u)_m$, where $(\tau u)_m$ is the total power loss over the period of the swash cycle. Obviously, for symmetric flow we would have $(\tau u)^+ = (\tau u)^- = \frac{1}{2}(\tau u)_m$. However, the forward flow velocities exceed the reverse flow velocities [7], and the power losses are also asymmetric,

$$(\tau u)^+ = \tfrac{1}{2}(\tau u)_m (1+a), \quad (\tau u)^- = \tfrac{1}{2}(\tau u)_m (1-a)$$

($a < 1$ is the measure of asymmetry). Now relations (4) are written in the form

$$q_R^+ = \frac{\varepsilon_b}{2\tan\phi}(\tau u)_m \frac{1+a}{1+b},$$

$$q_R^- = \frac{\varepsilon_b}{2\tan\phi}(\tau u)_m \frac{1-a}{1-b}, \qquad (5)$$

$$b = \frac{\beta}{\tan\phi},$$

and the resulting flow rate $\hat{q}_R = q_R^+ - q_R^-$ is defined as

$$\hat{q}_R = \frac{\varepsilon_b}{\tan\phi}(\tau u)_m (a-b) \qquad (6)$$

(assumed to be $b^2 \ll 1$).

As can be seen, $\hat{q}_R = 0$, if $a - b = 0$ or $a\tan\phi - \beta = 0$. Since the zero value of $\hat{q}_R$ corresponds to the stable (equilibrium) state of the bottom, the value of $a\tan\phi$ can be interpreted as the equilibrium beach slope β_{eq}. This allows us to write $a - b = \beta_{eq} - \beta$. If the beach slope is greater than the equilibrium beach slope ($\beta_{eq} - \beta < 0$), then material is transported to the underwater slope ($\hat{q}_R < 0$), and in the case of $\beta_{eq} - \beta > 0$, sediment is transported to the beach ($\hat{q}_R > 0$).

We characterize the magnitude of the swash flow velocity by the value $u_R = \sqrt{2gR}$, where g is the acceleration of gravity, R is the runup height above the still water level (Fig. 1a). Since $\tau \sim \rho u^2$, then $(\tau u)_m \sim \rho u_R^3$. As a result, the volumetric sediment discharge, expressed in $m^3/(m\ s)$, will be determined from (6) as

$$\hat{q}_R = K_R \mu\rho(2gR)^{3/2}(\beta_{eq} - \beta), \ \mu = [g(\rho_g - \rho)]^{-1}. \quad (7)$$

Here K_R is a model calibration parameter of order 10^{-3} including all constant coefficients. The multiplier μ translates the immersed weight of the sediment into its volume, ρ is the density of water, ρ_g is the density of solids, and p is the porosity of the sediment.

To determine the runup height, we use the well-known formula [22], which is based on field data and can be written in the form [6]:

$$R = \left(0.385^2 + 0.55\sqrt{0.563^{2\ 2} + 0.004}\right)\sqrt{H_{s0}L_0}\cos^{1/4}\Theta_0, \quad (8)$$

Where H_{s0} and $L_0 = \left(\frac{g}{2\pi}\right)T_p^2$ are significant wave height and wavelength in deep water (T_p is the peak period of the wave spectrum), Θ_0 is the angle between the wave ray and the normal to the shore (at $\Theta_0 < 45°$ the effect of the angle of wave approach is almost negligible).

To estimate the equilibrium beach slope, we take as a basis the well-known formula [23], including a calibration factor $K\beta$ of order 1:

$$\beta_{eq} = 0.12K_\beta\left(\frac{T_p\sqrt{gd_g}}{H_{sB}}\right)^{0.5}, \qquad (9)$$

Where d_g is the average sand particle size, H_{sB} is the wave height at the breaking depth h_B. The latter corresponds to the breaking of waves of 1% cumulative exceedance height [3],

$$h_B = \left(\frac{1}{4\pi\gamma_B^2}\right)^{0.4} H_{1\%0}^{0.8}\left(gT_p^2\right)^{0.2}\left(\frac{\cos\Theta_0}{\cos\Theta_B}\right)^{0.4}, \qquad (10)$$

where Θ_B is the angle of approach of the waves at the breaking depth, and the collapse index $\gamma_B = \frac{H_{1\%B}}{h_B} = 0.8$. With Rayleigh distribution of wave heights we have $H_{1\%B} \approx 1.5H_{sB}$, and hence H_{sB} is related to h_B by the relation $H_{sB} \approx 0.53h_B$.

Adaptation of morphology to external influences

During a storm, the beach morphology adapts to external influences, which in turn affects the influences themselves. Due to the feedback between morphology and hydrodynamics, the morphodynamic system tends towards equilibrium. In the context of our model, this means that the initial beach slope β_0 should tend towards the value β_{eq}. This situation is described by an equation of the form

$$\frac{d\beta}{dt} = \lambda\left(\beta_{eq} - \beta\right), \qquad (11)$$

where the value λ characterizes the speed of the process. From the solution of this equation it follows that after the time interval Δt the beach slope reaches the value of

$$\beta(\Delta t) = \beta_{eq} - (\beta_{eq} - \beta_0)e^{-\lambda\Delta t}. \qquad (12)$$

To simplify the task, in further calculations we use the average for the time Δt value of slope, defined as

$$\overline{\beta} = \tfrac{1}{2}\left(\beta_0 + \beta(\Delta t)\right) \cdot \quad (13)$$

As shown in [19], the beach dynamics is closely related to the evolution of the underwater bar in the wave breaking zone, and the time scale of morphological changes in both cases should be approximately the same. It was found that the volume of the bar under the influence of waves changes in accordance with the dependence similar to (11), and the value λ is parameterized in the form of

$$\lambda = \frac{\lambda_0}{\Omega_s^{1/2}}, \quad \Omega_s = \frac{H_{s0}}{wT_p}, \quad (14)$$

where Ω_s is the Dean parameter, w is the settling velocity of solid particles (depending on their size), and the value λ_0 is estimated on the basis of experiments in the wave channel as 0.15 h^{-1} [19]. In further, assuming the correspondence of the rates of morphological changes of the beach and the underwater bar, we will use relations (14) in the calculations.

CALIBRATION OF THE MODEL BASED ON LABORATORY EXPERIMENTS

Published data from wave channel experiments were used to calibrate the model and are summarized in Table 1. During the experiments, irregular waves with constant parameters affected initially linear sand profiles. In [15] and [26], plots of bottom profiles before and after wave action are given, from which changes in the volume of the overwater beach were calculated $V_b^{(m)}$, and in [14] directly measured values are given $V_b^{(m)}$.

During calibration, it was found that the values of the coefficient K_R in the sediment discharge formula (7) are different for erosion and accumulation conditions. As a result, the optimal values of the coefficients were determined as follows:

$$K_\beta = 0.65,$$
$$K_R = \begin{cases} 0.0015, \ \beta_0 > \beta_{eq}, \ \text{erosion} \\ 0.002, \quad \beta_0 < \beta_{eq}, \ \text{accumulation} \end{cases} \quad (15)$$

The calculated changes in beach volume $V_b^{(c)}$ are given in the last column of Table 1. Their comparison with the observed data is shown in Fig. 2. The RMSE $= \sqrt{\dfrac{\sum_j \left(V_{bj}^{(m)} - V_{bj}^{(c)}\right)^2}{n}}$ is 0.31 m^3/m (n – total number of tests).

MODEL VERIFICATION BASED ON FIELD DATA

Two types of sandy shores are distinguished, one of which is characterized by a developed system of underwater bars, while the shores of the second type reveal either single bar or have none at all. The storm changes of the beach observed on the shores of the second type are significantly larger [2]. Therefore, it makes sense to perform model verification separately for each type of shore. Further, published observation

Table 1. Experimental conditions in wave channels and comparison of measured ($V_b^{(m)}$) and calculated ($V_b^{(c)}$) changes in overwater beach volume

Test	d_g, mm	β_0	H_{s0}, m	T_p, c	T_w, h	$V_b^{(m)}$, m^3/m	$V_b^{(c)}$, m^3/m
Erosion profiles							
Delft20 [26]	0.13	0.050	0.167	2.33	24	–0.06	0.08
Delft15 [26]	0.13	0.067	0.167	2.33	24	–0.11	–0.16
Delft10 [26]	0.13	0.100	0.167	2.33	24	–0.25	–0.80
Barc15 [26]	0.25	0.067	0.53	4.1	22.9	–1.1	–1.15
Hann15 [26]	0.27	0.067	0.97	5.6	32.8	–4.4	–4.48
Wise1 [15]	0.25	0.067	0.47	3.7	4.0	–0.20	–0.30
115E1 [14]	0.25	0.067	0.45	3.5	3.0	–0.19	–0.21
115E2 [14]	0.25	0.067	0.55	3.5	3.0	–0.48	–0.30
SB0 [14]	0.33	0.067	0.80	6.0	20	–2.75	–2.35
Accumulation profiles							
115A1 [14]	0.25	0.067	0.25	5.2	10	0.20	0.13
125A1 [14]	0.25	0.040	0.25	5.2	10	0.20	0.97
SBA1 [14]	0.33	0.067	0.60	12	6	0.28	0.23

materials are used, which record storm chronograms (changes in the parameters H_s and T_p in time), as well as bottom profiles before the beginning and after the end of the storm.

It should be noted that storm impacts were accompanied by fluctuations in the sea level due to tide and surge, which were not included in the calculations. Wave direction could also change during the storm, but due to the lack of information about this in the sources used, waves were considered as normal to the shore. Unaccounted for factors could lead to additional calculation errors.

Shores with a system of underwater bars

The conditions of observations and the results of model testing are shown in Table 2. The column "Storm" shows the name of the wave file corresponding to the time of observations (month and year). The storm duration T_w and the time step Δt, with which the calculations were performed, are further marked. The values of $V_b^{(m)}$ were estimated based on a comparison of plots of the initial and final coastal profiles recorded before and after the storm. The slope β_0 was defined as the ratio of maximum beach elevation to the beach width.

Views of the profiles before and after the storm are shown in Fig. 3. The Duck profiles refer to the Atlantic coast of the USA, while the Skallingen and Egmond profiles refer to the Danish and Dutch shores of the North Sea. In the Duck profiles, the average sand size in the overwater portion of the beach ranged from 0.2 to 2 mm [17], and $d_g = 1$ mm was taken as a representative value.

Fig. 4a reflects the recorded storm scenarios. Fig. 4b shows the calculated changes in beach volume and slope during the storm. As can be seen, during the wave intensification phase, erosion increases and beach slope decreases. As the waves decay, the beach volume and slope tend to the pre-storm state.

From Table 2 and Fig. 3 it follows that the observed final storm deformations of the beach are very small. The calculated values $V_b^{(c)}$ also do not go beyond the first cubic meters per meter of beach length, i.e., they

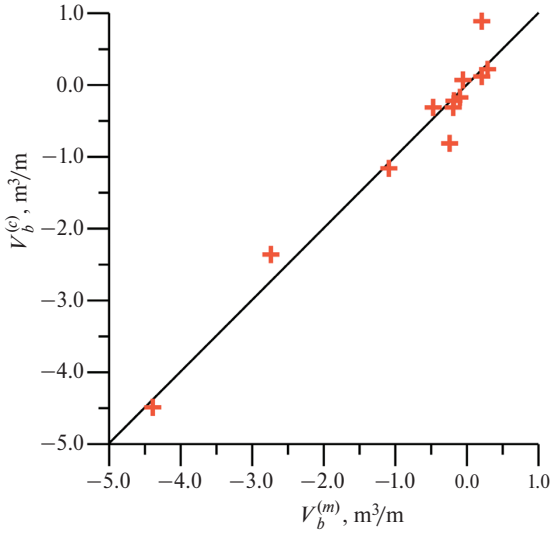

Fig. 2. Changes in the beach volume according to the data of experiments in wave channels ($V_b^{(m)}$) and according to the results of calculations ($V_b^{(c)}$) using the accepted values of calibration coefficients according to (15).

appear to be of the same order as the recorded changes in volumes $V_b^{(m)}$.

Shores with no or only one submerged bar

The source of data for testing the model was the study [27], which contains chronograms of storms and corresponding deformations of bottom profiles observed in different areas of the Atlantic coast of the USA. The conditions and results of the observations are characterized in Table 3.

The shores under consideration are composed of medium-grained sand and are characterized by beach slopes of 0.04÷0.08. Changes in the volume of the overwater beach $V_b^{(m)}$ were determined by comparing plots of coastal profiles before and after the storm, examples of which are shown in Fig. 5.

As can be seen in Table 3, storm deformation of beaches is measured in tens of cubic meters per meter of shore, an order of magnitude greater than for shore conditions with multiple-bar systems.

The storm scenarios labeled in Table 3 are shown in Fig. 6a, and the corresponding chronograms

Table 2. Observational conditions on shores with developed submerged bars and resulting storm-related changes in beach volume from observations ($V_b^{(m)}$) and calculations ($V_b^{(c)}$)

Profile	d_g, mm	β_0	Storm	T_w, h	Δt, h	$V_b^{(m)}$, m³/m	$V_b^{(c)}$, m³/m
Duck-82 [17]	1.0	0.080	Dec-82	192	6	-10^0	−2.3
Duck-84 [17]	1.0	0.089	Apr-84	72	3	10^0	−1.5
Skallingen [8]	0.2	0.042	Oct-95	78	3	-10^0	−1.1
Egmond [25]	0.3	0.022	Oct-98	168	3	$\pm 10^0$	−3.1

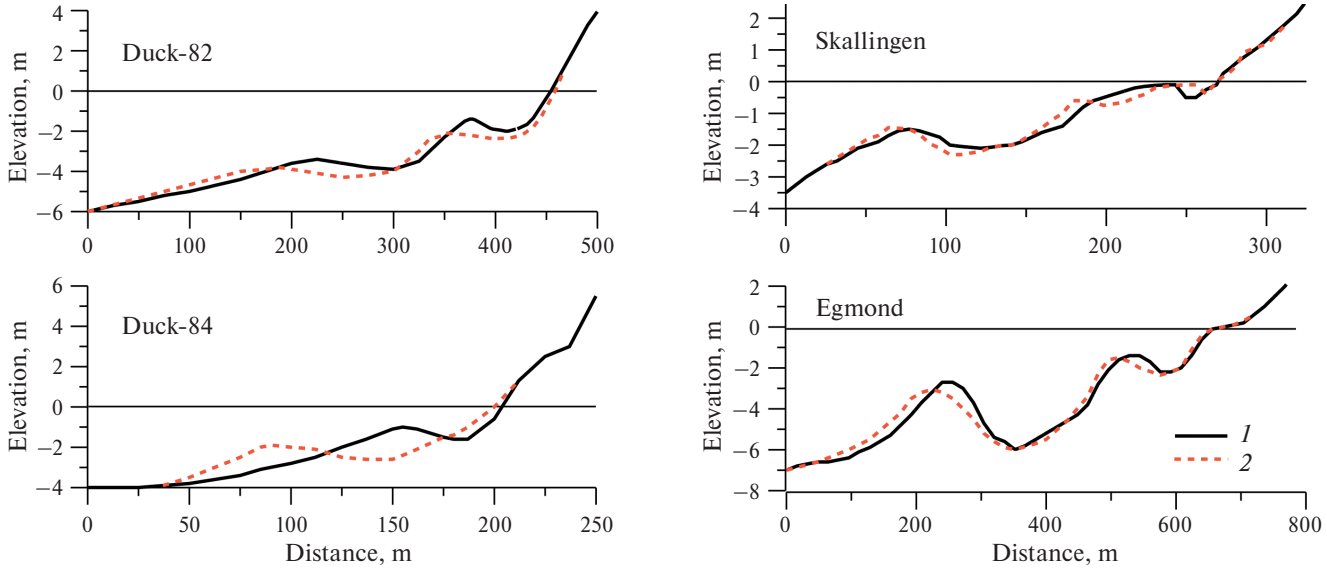

Fig. 3. Coastal profiles with underwater bar systems before the storm (*1*) and after the storm (*2*) according to [8, 17, 25].

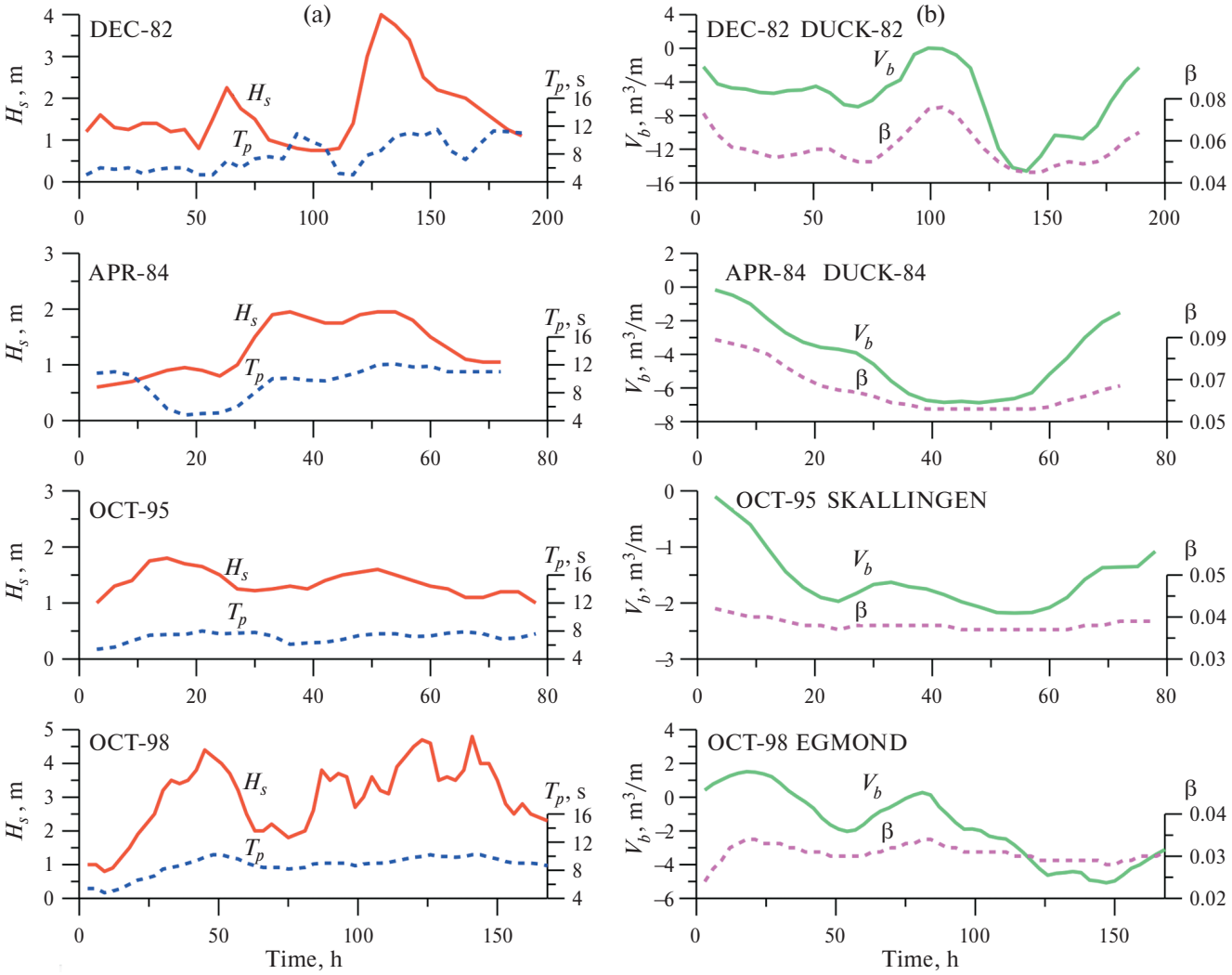

Fig. 4. Storm chronograms (a) and corresponding calculated changes in beach volume and slope (b) on shores with submerged bar systems.

of changes in beach volume and slope are shown in Fig. 6b. As can be seen, storms cause significant beach erosion during the wave growth phase, which is not compensated for by accumulation during wave attenuation.

As calculations have shown, for beach erosion conditions the calibration factor K_R, determined by relation (15), should be doubled. In other words, in the case of $\beta_0 > \beta_{eq}$, when calculating the values of $V_b^{(c)}$, given in Table 3 and Fig. 6b, the value $K_R = 0.003$ was used. The RMSE was 9.6 m^3/m, which corresponds to 24% of the mean recorded change in beach volume.

The result of two consecutive storms

Works [27] and [28] present data on erosion volumes on the coast of Ocean City (Maryland) under the action of two consecutive storms that occurred in November 1991 and January 1992 (Nov-91 and Jan-92) and had durations of 96 and 90 h, respectively. Table 4 is synthesized from these data and shows the beach characteristics and resulting changes in beach volume recorded on a number of profiles. The calculated scour volumes for the first and second storms separately $\left(V_{b1}^{(c)} \text{ and } V_{b2}^{(c)}\right)$ and their sum $\left(V_b^{(c)}\right)$ are also shown here.

Ocean City bottom profiles are characterized by a single submarine berm and are exemplified by the OC37 profile shown in Fig. 5.

Fig. 7a shows the Nov-91 and Jan-92 sequential storm scenarios, and Fig. 7b shows the calculated changes in beach volume and slope for profile 63St. On the other profiles, the changes V_b and β are similar in nature.

In calculations of the second storm, the initial beach slope was assumed to be equal to the slope generated by the first storm. In the situations $\beta_0 > \beta_{eq}$, as before, the calibration factor K_R=0.003 was used.

Table 3. Observational conditions on shores without or with a single bar [27] and resulting storm-related changes in beach volume from observations ($V_b^{(m)}$) and calculations ($V_b^{(c)}$).

Profile	d_g, mm	β_0	Storm	T_w, h	Δt, h	$V_b^{(m)}$, m^3/m	$V_b^{(c)}$, m^3/m
M1	0.40	0.060	Mar-84	192	6	–36	–34.8
M9	0.40	0.060	Mar-84	192	6	–25	–34.8
P8	0.40	0.075	Mar-84	192	6	–40	–45.1
DEB	0.35	0.042	Sep-89	60	3	–45	–32.7
MYB	0.35	0.050	Sep-89	60	3	–42	–36.5
OC37	0.35	0.075	Oct-91	174	3	–32	–33.3
DB100	0.33	0.067	Dec-92	144	3	–50	–26.1
RB214	0.35	0.080	Dec-92	144	3	–48	–39.3

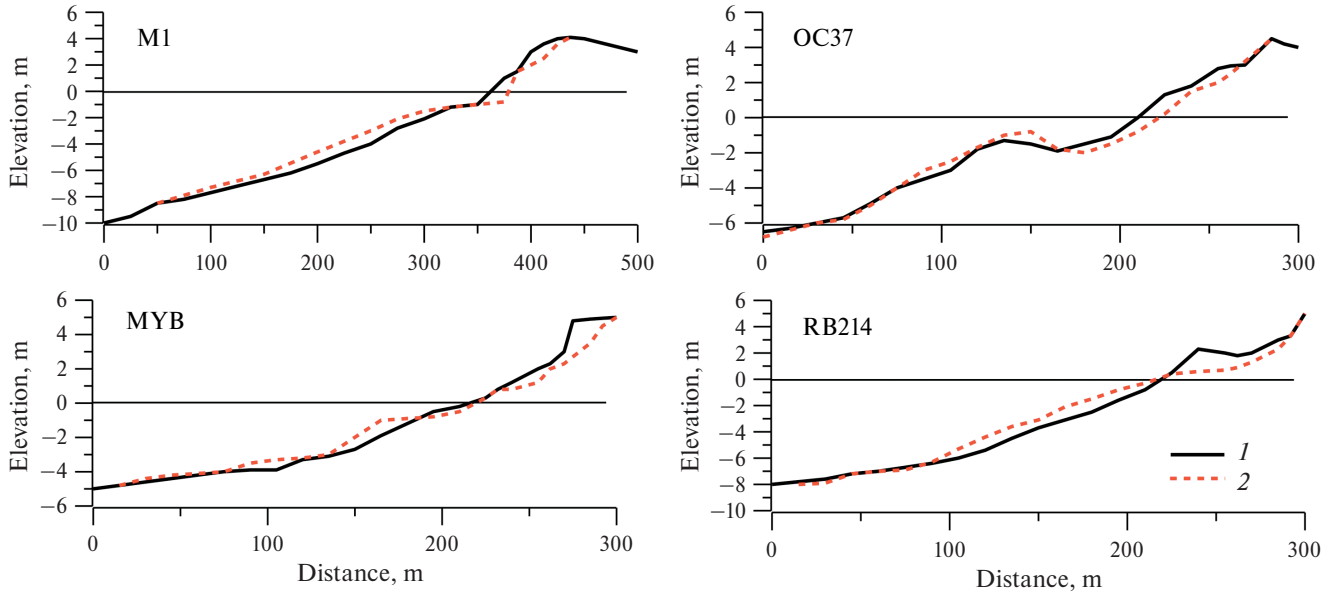

Fig. 5. Examples of coastal profiles without bars or with one bar before (*1*) and after the storm (*2*) according to [27].

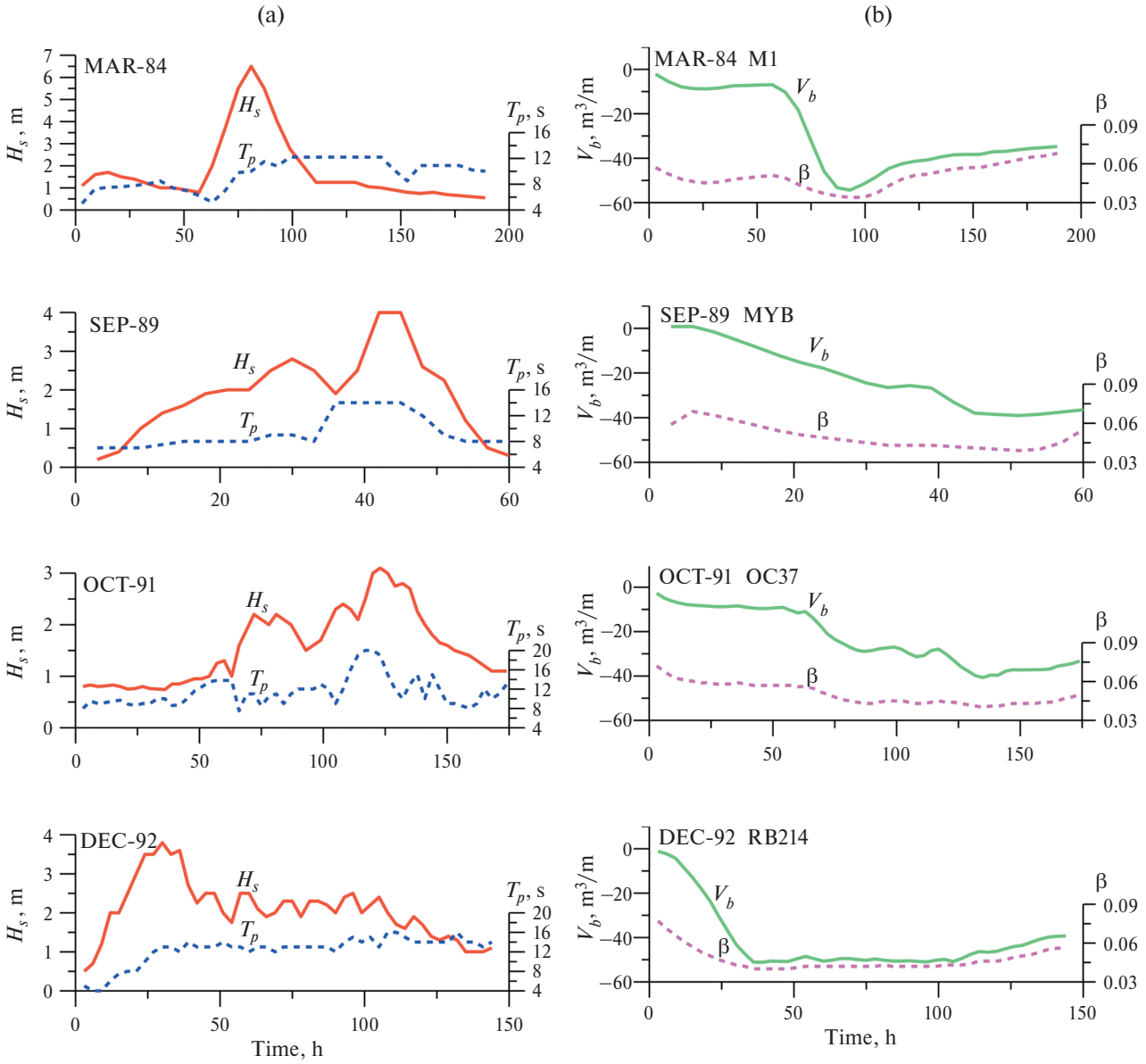

Fig. 6. Storm chronograms (a) and calculated changes in beach volume and slope (b) on shores without or with a single bar.

Table 4 and Fig. 7b show that the main contribution to beach scour was made by the first storm. The beach slope generated by the first storm was close to the optimum value. As a result, the volume of material carried away by the second storm was only about a quarter of the total scour volume.

The calculated and measured final scour volumes are in satisfactory agreement with each other. The RMSE = 4.9 m³/m, which is 11% of the average scour volume.

DISCUSSION OF RESULTS

One of the key parameters of the model under consideration is the beach slope. Its optimum value decreases with increasing wave height. Therefore, during storm development, the slope tends to decrease, which is supported by the transport of beach material onto the underwater slope. In the attenuation phase of the storm, the slope tends to increase, which is achieved by the transportation of additional amounts of material from the underwater slope to the beach. However, beach adaptation occurs with a certain time lag. This feature is simulated in our model using the algorithm proposed by Larson et al. [19] to predict changes in the volume of the underwater bar in the breaking zone. The time scales of both processes appear to be close to each other.

Testing of the model on the basis of laboratory experiments shows that the recommended

Table 4. Observed and calculated changes in beach volume as a result of two consecutive storms (observational data [27, 28])

Profile	d_g, mm	β_0	$V_b^{(m)}$, m³/m	$V_{b1}^{(c)}$, m³/m	$V_{b2}^{(c)}$, m³/m	$V_b^{(c)}$, m³/m
37St	0.33	0.08	–48	–29.7	–9.5	–39.2
52St	0.35	0.09	–46	–35.2	–9.5	–44.7
63St	0.37	0.09	–44.8	–33.5	–9.4	–42.9
74St	0.38	0.09	–50.0	–32.8	–9.7	–42.5
103St	0.40	0.09	–42.4	–31.3	–9.1	–40.4
124St	0.40	0.09	–40.1	–31.3	–9.1	–40.4

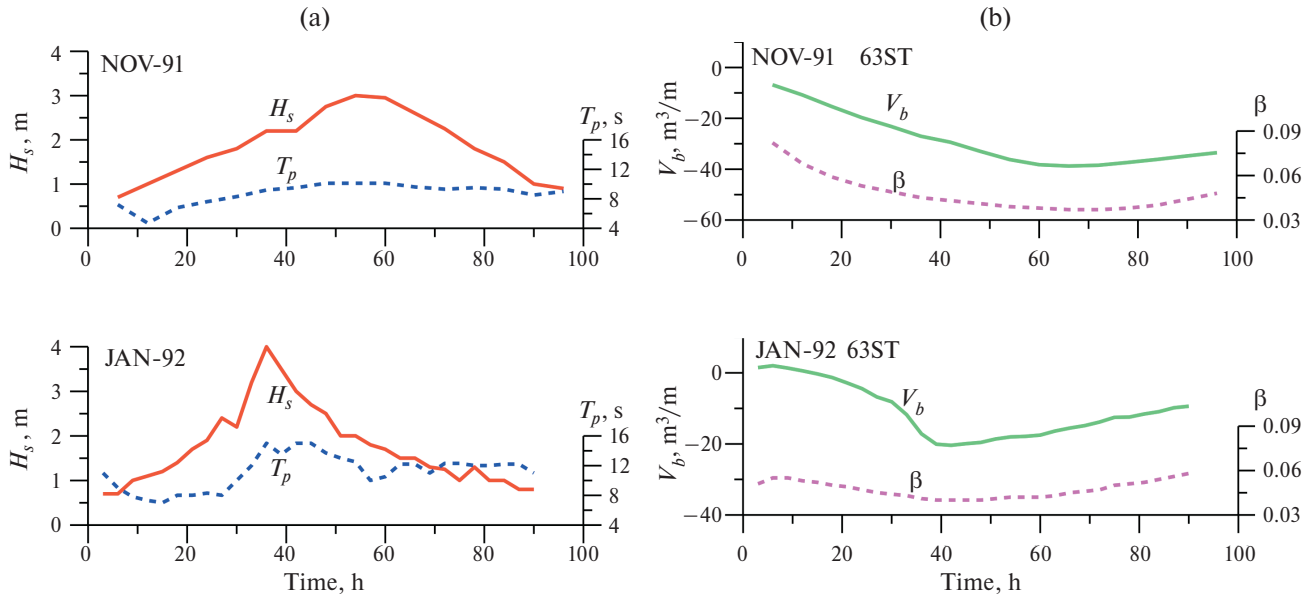

Fig. 7. Storm chronograms (a) and calculated changes in beach volume and slope (b) for two consecutive storms Nov-91 and Jan-92.

combination of calibration coefficients $K\beta$ and K_R provides acceptable agreement of calculations with observational data. The values of K_R for erosion conditions ($\beta_0 > \beta_{eq}$) are somewhat smaller than for accumulation conditions ($\beta_0 < \beta_{eq}$).

The found values of the coefficients $K\beta$ and K_R are also applicable to natural beaches, but not for all types of coastal morphology. Testing the model on the basis of field data leads to the conclusion that the beach erosion rate depends significantly on the type of coastal profile. Profiles with a developed system of submerged bars exhibit relatively weak beach change even during strong and prolonged storms. However, on shores with no or a single bar, storm scour is measured in tens of cubic meters per meter of beach. This difference should be taken into account in the calculations by using different values of the calibration factor K_R. Its value can be characterized as follows:

$\beta_0 < \beta$ accumulation: K_R=0.002,

$\beta_0 > \beta$ erosion

$$K_R = \begin{cases} 0.015, \text{profile with a system} \\ \quad\quad\quad\quad \text{of submerged bars,} \\ 0.003, \text{profile with no or a single berm.} \end{cases} \quad (16)$$

As noted above, sea level fluctuations during a storm were not included in the calculation. In essence, the average beach slope determined by our model was assumed to be independent of the current mean water level. It was assumed that the level does not

reach a position where overflow over the crest of the beach berm is possible. Modeling of overflow situation is considered, for example, in [4] and [19].

Changes in beach volume can also be caused by gradients in longshore sediment transport, as illustrated by the data presented in [28]. However, this factor does not appear to have played a decisive role in the examples of storm-induced beach changes used to verify the model. The computational results show satisfactory agreement with the data obtained both on shores with multiple-bar systems and on profiles without bars. In the latter case, the RMS error of the calculations did not exceed 24% of the mean value of beach volume changes. And when modeling the impact of two consecutive storms, the error was only 11%.

The issue of shoreline displacements during a storm is of practical interest. According to formula (2) and Fig. 1b, during the time Δt the shoreline should move by the distance $\Delta x_b = \Delta V_b/R$. However, for a realistic assessment of shoreline displacement, it is necessary to take into account changes in the volume of not only the overwater beach but also its underwater part. Such a task must be solved on the basis of a more complex model that incorporates the action of wave mechanisms and changes in the bottom profile during the storm.

CONCLUSION

This approach to assessing storm-related changes in beach volume is based on a model of sediment transport in the wave swash zone developed by the author. The model input parameters are sand size, beach slope and a storm scenario including a chronogram of wave heights and periods.

The resulting sediment discharge on the beach is the result of imbalance between the asymmetry of the swash flow and gravity. The direction of transport is determined by the sign of the difference between the current beach slope and the slope at equilibrium.

Calibration and verification of the model show that beach erosion and accumulation processes are characterized by different rates, which also depend on the type of coastal profile. Thus, storm erosion on shores without submerged bars can be an order of magnitude greater than on shores with multiple-bar systems.

During a storm, the slope of the beach tends to an equilibrium value that corresponds to the current wave action. As the wave intensifies, the slope decreases, accompanied by a decrease in beach volume due to the transport of material to the underwater slope, and as the storm subsides, the slope and beach volume increase.

Beach recovery to the prestorm volume was only observed on profiles with multiple-bar systems and was not observed on profiles without bars.

In the case of two successive storms of approximately equal strength, the major contribution to beach change is made by the first of these storms.

The results of the calculations agree satisfactorily with the data of field observations. The RMS error of the calculations ranges from 11 to 24% with respect to the average value of the recorded changes in beach volume.

FUNDING

The work was carried out within the framework of the state assignment of IO RAS (theme No. FMWE-2024-0018).

CONFLICT OF INTERESTS

The author of this paper declares that he has no conflict of interests.

REFERENCES

1. *Leontiev I.O.* Coastal dynamics: waves, currents, sediment fluxes. M.: GEOS, 2001. 272 p.
2. *Leontiev I.O.* Morphodynamic processes in the coastal zone of the sea. LAP LAMBERT Academic Publishing. Saarbrücken, 2014. 251 p.
3. *Leontiev I.O.* About calculation of longshore sediment transport // Oceanology. 2014. Vol. 54. No. 2. pp. 226–232. DOI: 10.7868/S0030157414020130
4. *Leontiev, I.O.; Ryabchuk, D.V.; Sergeev, A.Yu.* Modeling of storm deformations of a sandy shore (on the example of the eastern part of the Gulf of Finland) // Oceanology. 2015. Vol. 55. No. 1. pp. 147–158. DOI: 10.7868/S0030157414060069
5. *Leontiev, I.O.*Assessment of the hazard of storm scouring of a sandy shore // Oceanology. 2021. Vol. 61. No. 2. pp. 286–294. DOI**:** 10.31857/S0030157421020118
6. *Leontiev I.O.* Abrasion of the shore composed by loose material // Oceanology. 2022. Vol. 62. No. 1. pp. 125–134. DOI: 10.31857/S0030157422010087
7. *Longinov V.V.* Dynamics of the coastal zone of non-tidal seas. Moscow: Izd. of the USSR Academy of Sciences, 1963. 379 p.
8. *Aagaard T., Nielsen J., Greenwood B.* Suspended sediment transport and nearshore bar formation on a shallow intermediate-state beach // Marine Geology. 1998. Vol. 148. pp. 203–225.
9. *Bagnold R.A.* Mechanics of marine sedimentation // The Sea. V. 3. N.-Y.: Wiley, 1963. pp. 507–528.

10. *Baldock T., Alsina J., Càceres I. et al.* Large-scale experiments on beach profile evolution and swash zone sediment transport induced by long waves, wave groups and random waves // Coastal Engineering. 2011. Vol. 58. pp. 214–227.
11. *Blenkinsopp C.E., Turner I.L., Masselink G., Russell P.E.* Swash zone sediment fluxes: field observations // Coastal Engineering. 2011. Vol. 58. pp. 28–44.
12. *Càceres I., Alsina J.M.* Suspended sediment transport and beach dynamics induced by monochromatic conditions, long waves and wave groups // Coastal Engineering. 2016. Vol. 108. pp. 36–55. https://doi.org/10.1016/j.coastaleng.2015.11.004.
13. *Chardón-Maldonado P., Pintado-Patiño J.C., Puleo J.A.* Advances in swash-zone research: small-scale hydrodynamic and sediment transport processes // Coastal Engineering. 2016. Vol. 115. pp. 8–25. https://doi.org/10.1016/j.coastaleng.2015.10.008.
14. *Chen W., van der Werf J.J., Hulcsher S.J.M.H.* Practical modelling of sand transport and beach profile evolution in the swash zone // Coastal Engineering. 2024. Vol. 191.
15. *Eichentopf S., Càceres I., Alsina J.M.* Breaker bar morphodynamics under erosive and accretive wave conditions in large-scale experiments // Coastal Engineering. 2018. Vol. 138. pp. 36–48. https://doi.org/10.1016/j.coastaleng.2018.04.010
16. *Karambas T.V.* Prediction of sediment transport in the swash-zone by using a nonlinear wave model // Continent. Shelf Res. 2006. Vol. 26. pp. 599–609.
17. *Larson M., Kraus N.C.* SBEACH: numerical model for simulating storm-induced beach change. Tech. Rep. CERC-89–9. 1989. US Army Eng. Waterw. Exp. Station. Coastal Eng. Res. Center.
18. *Larson M., Kubota S., Erikson L.* Swash-zone sediment transport and foreshore evolution: field experiments and mathematical modeling // Mar. Geol. 2004. Vol. 212. pp. 61–79.
19. *Larson M., Palalane J., Fredriksson C., Hanson H.* Simulating cross-shore material exchange at decadal scale. Theory and model component validation // Coastal Engineering. 2016. Vol. 116. pp. 57–66. https://doi.org/10.1016/j.coastaleng.2016.05.009.
20. *Leont'yev I.O.* Numerical modelling of beach erosion during storm event // Coastal Engineering. 1996. Vol. 47. pp. 413–429.
21. *Leont'yev I.O., Akivis T.M.* Erosion Index for Assessing Vulnerability of Sandy Beach // Processes in GeoMedia – V. VI. VI. Springer Geology / T. Chaplina (ed.). 2023. pp 19–32.
22. *Stockdon H.F., Holman R.A., Howd P.A., Sallenger A.H.* Empirical parameterization of setup, swash, and runup // Coastal Engineering. 2006. Vol. 53. pp. 573–588.
23. *Sunamura T.* Sandy beach geomorphology elucidated by laboratory modeling // Applications in coastal modeling / Eds. Lakhan V.C., Trenhail A.S. Amsterdam: Elsevier, 1989. pp. 159–213.
24. *Van Rijn L.C.* Prediction of dune erosion due to storms // Coastal Engineering. 2009. Vol. 56. pp. 441–457. https://doi.org/10.1016/j.coastaleng.2008.10.006.
25. *Van Rijn L.C., Walstra D.J.R., Grasmeier B., Sutherland J., Pan S., Sierra J.P.* The predictability of cross-shore bed evolution of sandy beaches at the time scale of storms and season using process-based profile models // Coastal. Engineering. 2003. Vol. 47. pp. 295–327.
26. *Van Rijn L.C., Tonnon P.K., Walstra D.J.R.* Numerical modelling of erosion and accretion of plane sloping beaches at different scales // Coastal Engineering. 2011. Vol. 58. pp. 637–655.
27. *Wise A., Smith S.J., Larson M.* SBEACH: numerical model for simulating storm-induced beach change. Tech. Rep. CERC-89–9. Report 4: Cross-shore transport under random waves and model validation with supertank and field data. US Army Corps of Engineers. 1996.
28. *Zheng J., Dean R.G.* Numerical models and intercomparisons of beach profile evolutions // Coastal Engineering. 1997. Vol. 30. pp. 169–201.